

Supporting Information

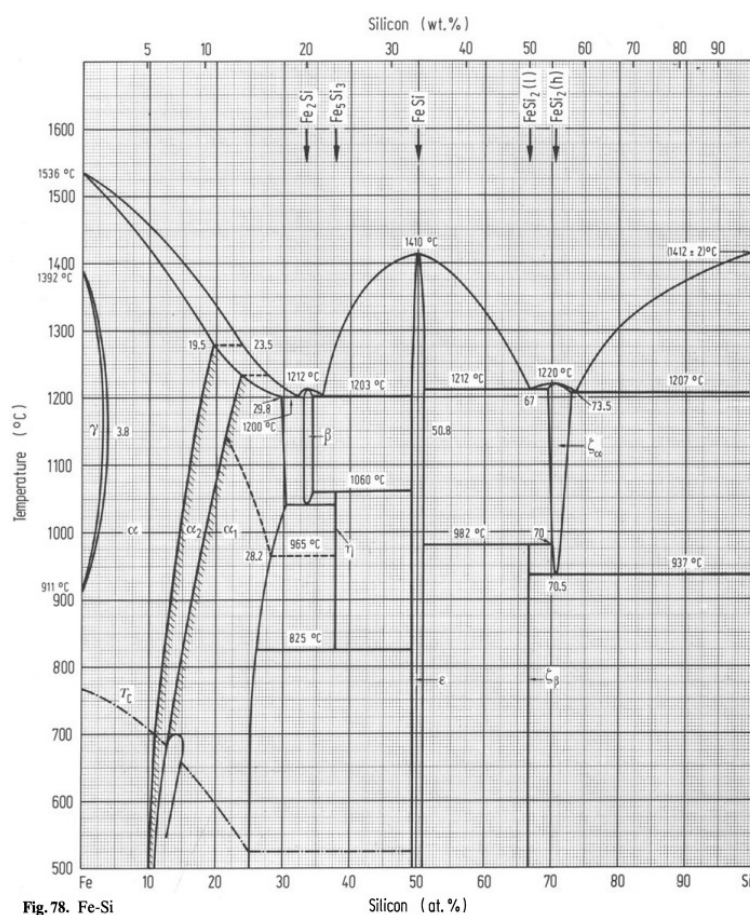


Figure S1. Fe-Si binary phase diagram. Reprinted with permission from ref 41. Copyright 1982 Springer-Verlag Berlin Heidelberg.

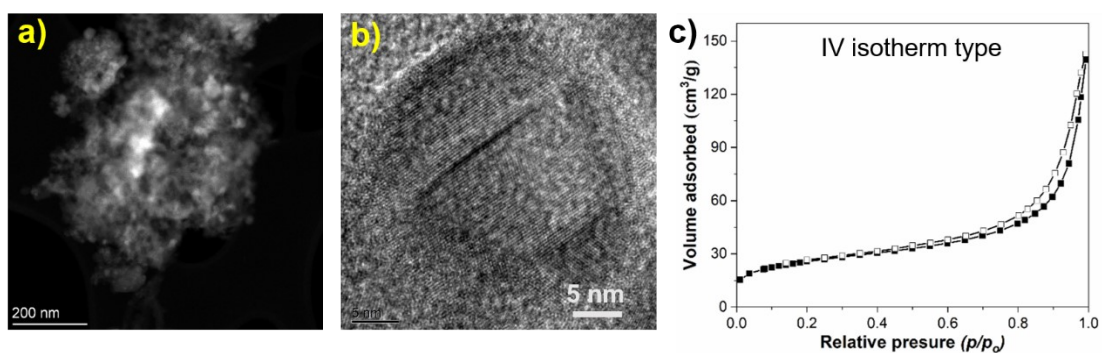


Figure S2. a) STEM images of FeSi NPs; b) HRTEM images of FeSi NPs; c) N₂ adsorption and desorption isotherm of porous FeSi NPs.

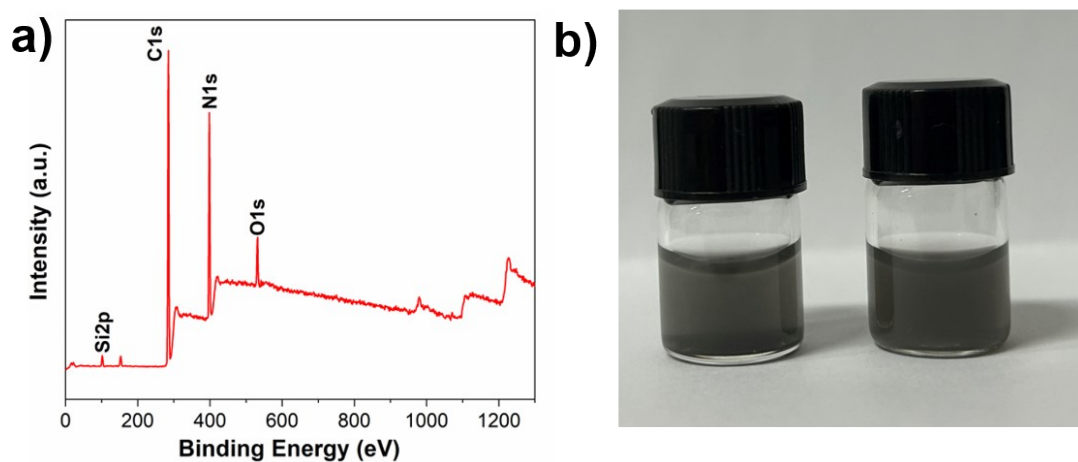


Figure S3. a) XPS survey spectrum of FeSi@PEI NPs; b) Photographs of FeSi NPs (left) and FeSi@PEI NPs (right) aqueous suspensions taken just after ultrasound.



Figure S4. Photographs of 5 μL FeSi@PEI NPs (5 mg/mL) in 495 μL PBS suspensions at six different pH values of 8, 7, 6, 5, 4 and 3 from left to right, taken just being treated (1st row) and 6 h after the treatment (2nd row) by ultrasonic cell crusher.

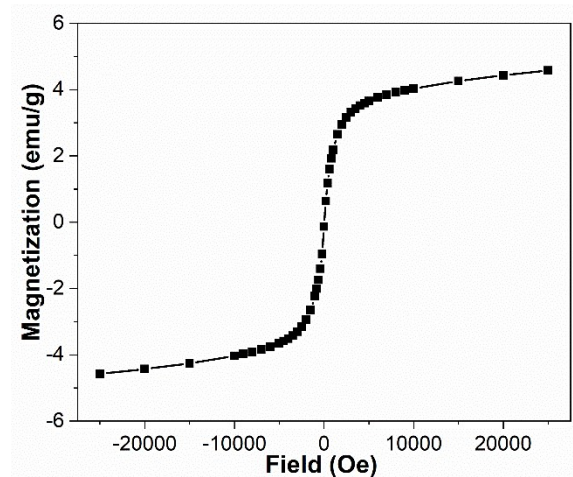


Figure S5. Magnetization curves of fabricated FeSi nanoparticles measured at room temperature.

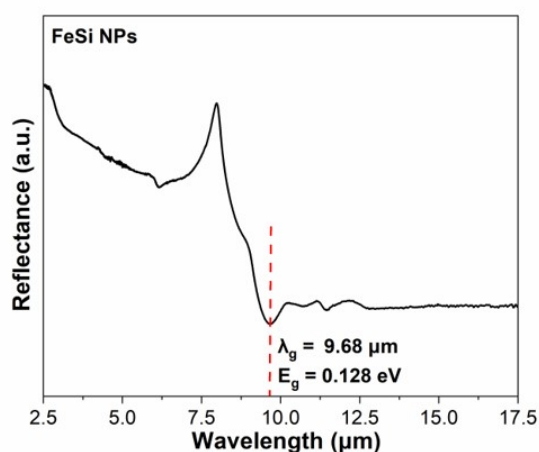


Figure S6. Narrow FTIR reflectance spectrum from 2.5 μm to 17.5 μm and the corresponding absorption threshold of FeSi NPs.

Table S1. Comparison of photothermal materials with photothermal efficiency (η) measured at various conditions.

<i>Materials</i>	<i>Solution concentrations</i>	<i>Wavelength</i>	<i>Power density</i>	<i>Irradiation time</i>	η	<i>References</i>
<i>Pd NPs</i>	50 $\mu\text{g/mL}$	808 nm	8 W/cm^2	30 min	93%	Nanoscale 2014, 6, 4345
<i>CuFeSe₂ NPs</i>	50 $\mu\text{g/mL}$	808 nm	0.75 W/cm^2	15 min	82%	ACS Nano 2017, 11, 5633–5645
<i>Au bellflowers</i>	-	808 nm	1 W/cm^2	5 min	74%	J. Am. Chem. Soc. 2014, 136, 8307–8313.
<i>CuCo₂S₄ NPs</i>	50 $\mu\text{g/mL}$	915 nm	0.189 W	5 min	73%	Adv. Funct. Mater. 2017, 27, 1606218
<i>cobalt</i>	40 $\mu\text{g/mL}$	808 nm	0.7 W/cm^2	5 min	70%	Nanoscale 2018, 10, 14190

<i>sulfide</i>						
<i>Au nanocages</i>	1.0*10 ¹⁰ particles/mL	808 nm	0.4 W/cm ²	10 min	64%	Angew. Chem. Int. Ed. 2013, 52, 4169–4173
<i>MoO_{3-x} NPs</i>	20 µg/ml	808 nm	1 W/cm ²	10 min	64%	J. Mater. Chem. B 2019, 7, 2032–2042
<i>Pd Nanosheets</i>	30 µg/mL	808 nm	1 W	10 min	52%	Small 2014, 10, 3139–3144
<i>Conjugated Polymer NPs</i>	10 µg/mL	1064 nm	0.9 W/cm ²	10 min	50%	ACS Appl. Mater. Interfaces 2018, 10, 7919–7926
<i>SiO_{0.92} NPs</i>	36 µg/mL of Si	1064 nm	1 W/cm ²	25 min	49%	Biomaterials 2017, 143 120–129
<i>Si NPs</i>	100 µg/ml	808 nm	1 W	10 min	34%	ACS Appl. Mater. Interfaces 2018, 10, 23529–23538
<i>FeSi NPs</i>	0.5 mg/mL	1064 nm	1 W/cm ²	10 min	76%	current work

The photothermal conversion efficiency (η) of FeSi at 1064 nm was calculated based on the following equations:

$$\eta = \frac{hs(T_{max} - T_{max, water})}{I(1 - 10^{-A_{1064}})} \quad (1)$$

$$hs = \frac{mC_p}{\tau_s} \quad (2)$$

$$\tau_s = -\frac{t}{\ln(\theta)} \quad (3)$$

$$\theta = \frac{T_{amb} - T}{T_{amb} - T_{max}} \quad (4)$$

where h is heat transfer coefficient, S is the surface area of the container, T_{max} is the equilibrium temperature of the sample solution after laser heating, $T_{max, water}$ is the equilibrium temperature of pure water under laser heating, I is the laser power, A_{1064} is the absorbance of the sample at 1064 nm. m is the mass of solution, C_p is specific heat capacity of solution.

The photothermal efficiency (η) was calculated as follows. For 200 µL aqueous dispersion of materials used in the measurement, the total mass (m) is 0.2 g; C_p of H₂O is 4.2 J/(g·°C); τ_s is 203.7 s determined from Figure 3e; A_{1064} is 0.9354 when the concentration of solids is 0.5 mg/mL; laser power (I) is 320 mW for 96-well plates of a 0.32 cm² surface area and a laser power density of 1 W/cm²; T_{max} is 80 °C; $T_{max, water}$ is 27.7 °C.

$$\eta = \frac{hs(T_{max} - T_{max, water})}{I(1 - 10^{-A_{1064}})} = \frac{0.2g \cdot (4.2J/g \cdot ^\circ C) \cdot (80 - 27.7)^\circ C}{203.7s \cdot 320mW(1 - 10^{-0.9354})} = 76.2\%$$